Article

Cell Reports

Regulation of Nuclear Hormone Receptors by MYCN-Driven miRNAs Impacts Neural Differentiation and Survival in Neuroblastoma Patients

Graphical Abstract

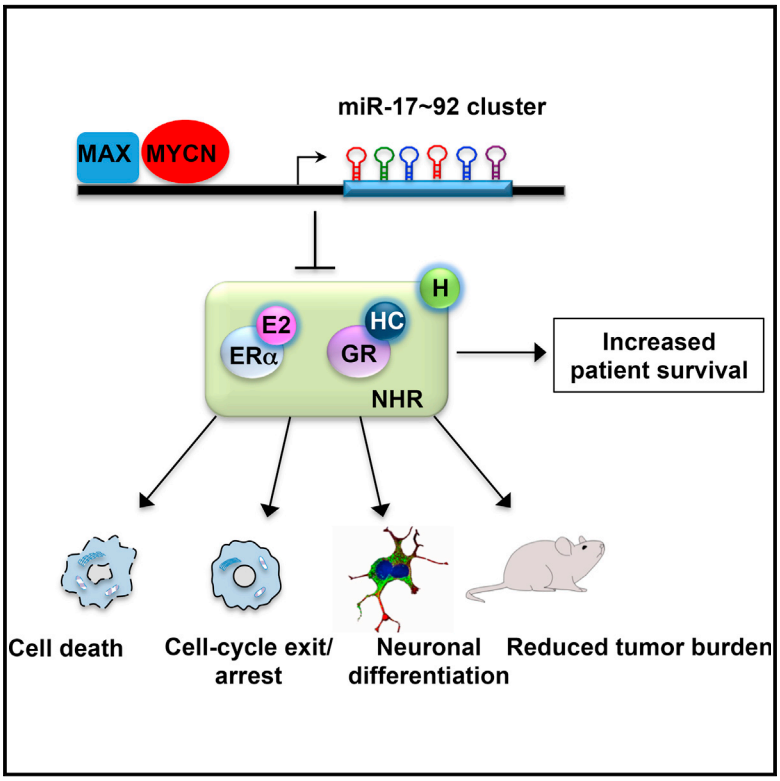

Highlights

- The MYCN-regulated miR-17∼92 cluster targets nuclear hormone receptors
- An NHR signature is associated with neural differentiation and patient survival
- The induction of MYCN or miR-17∼92 attenuates glucocorticoid receptor signaling
- Combined MYCN inhibition and GR activation drive differentiation and ease tumor burden

Authors

Diogo Ribeiro, Marcus D.R. Klarqvist, Ulrica K. Westermark, ..., Per Kogner, Jakob Lovén, Marie Arsenian Henriksson

Correspondence

diogo.ribeiro@ki.se (D.R.), marie.arsenian.henriksson@ki.se (M.A.H.)

In Brief

Ribeiro et al. show that expression of several nuclear hormone receptors is inhibited by the MYCN-regulated miR-17∼92 cluster in *MYCN*-amplified neuroblastoma. Furthermore, they demonstrate that activation of glucocorticoid signaling results in neural differentiation and reduced tumor burden. Together, these results suggest restoration of nuclear hormone signaling as a putative future therapy for neuroblastoma.

Ribeiro et al., 2016, Cell Reports *16*, 979–993
July 26, 2016
http://dx.doi.org/10.1016/j.celrep.2016.06.052

CellPress

Cell Reports
Article

OPEN ACCESS
CellPress

Regulation of Nuclear Hormone Receptors by MYCN-Driven miRNAs Impacts Neural Differentiation and Survival in Neuroblastoma Patients

Diogo Ribeiro,[1,*] Marcus D.R. Klarqvist,[1,4,5] Ulrica K. Westermark,[1,6] Ganna Oliynyk,[1] Johanna Dzieran,[1] Anna Kock,[2] Carolina Savatier Banares,[1] Falk Hertwig,[3] John Inge Johnsen,[2] Matthias Fischer,[3,7] Per Kogner,[2] Jakob Lovén,[1,8] and Marie Arsenian Henriksson[1,*]

[1]Department of Microbiology, Tumor and Cell Biology (MTC), Karolinska Institutet, 171 77 Stockholm, Sweden
[2]Childhood Cancer Research Unit, Department of Women's and Children's Health, Karolinska Institutet, 171 76 Stockholm, Sweden
[3]Department of Pediatric Oncology and Hematology, University Children's Hospital and Center for Molecular Medicine Cologne (CMMC), University of Cologne, 50931 Cologne, Germany
[4]Present address: Wellcome Trust Sanger Institute, Cambridge CB10 1SA, UK
[5]Present address: JDRF/Wellcome Trust Diabetes and Inflammation Laboratory, Department of Medical Genetics, Cambridge Institute for Medical Research, University of Cambridge, Cambridge CB2 0XY, UK
[6]Present address: Swedish Orphan Biovitrum AB, 112 76 Stockholm, Sweden
[7]Present address: Max-Planck-Institute for Metabolism Research, 50931 Cologne, Germany
[8]Present address: Third Rock Ventures, 29 Newbury Street, Boston, MA 02116, USA
*Correspondence: diogo.ribeiro@ki.se (D.R.), marie.arsenian.henriksson@ki.se (M.A.H.)
http://dx.doi.org/10.1016/j.celrep.2016.06.052

SUMMARY

MYCN amplification and MYC signaling are associated with high-risk neuroblastoma with poor prognosis. Treating these tumors remains challenging, although therapeutic approaches stimulating differentiation have generated considerable interest. We have previously shown that the MYCN-regulated miR-17∼92 cluster inhibits neuroblastoma differentiation by repressing estrogen receptor alpha. Here, we demonstrate that this microRNA (miRNA) cluster selectively targets several members of the nuclear hormone receptor (NHR) superfamily, and we present a unique NHR signature associated with the survival of neuroblastoma patients. We found that suppressing glucocorticoid receptor (GR) expression in MYCN-driven patient and mouse tumors was associated with an undifferentiated phenotype and decreased survival. Importantly, MYCN inhibition and subsequent reactivation of GR signaling promotes neural differentiation and reduces tumor burden. Our findings reveal a key role for the miR-17∼92-regulated NHRs in neuroblastoma biology, thereby providing a potential differentiation approach for treating neuroblastoma patients.

INTRODUCTION

Neuroblastoma is a childhood tumor that is believed to be caused by aberrations during normal development of the neural-crest-derived sympathoadrenal lineage (Maris, 2010). This disease exhibits heterogeneous clinical behavior, ranging from low-risk tumors, with a remarkable ability to differentiate and regress even with no or minimal therapy, to high-risk tumors responsible for the highest number of cancer-related deaths in infants (Brodeur, 2003). One of the few strong prognostic markers of adverse outcome is amplification of the *MYCN* gene, which has a prevalence of 40% in high-risk tumors and an overall survival of less than 50% (Brodeur, 2003; Maris, 2010). *MYCN* is normally expressed in the developing peripheral neural crest and sympathetic ganglia (Edsjö et al., 2004; Wakamatsu et al., 1997), and disruption of MYCN signaling leads to decreased proliferation and terminal differentiation of neuronal cells (Knoepfler et al., 2002). Interestingly, high-risk tumors without *MYCN* amplification frequently display elevated expression levels of MYC signature genes (Fredlund et al., 2008; Westermann et al., 2008), suggesting a prominent role for MYC signaling in aggressive neuroblastoma. It is well established that the MYC proteins upregulate the oncogenic miR-17∼92 microRNA (miRNA) cluster (Lovén et al., 2010; O'Donnell et al., 2005; Schulte et al., 2008). We have previously shown that miR-18a and miR-19a from this cluster inhibit the differentiation of neuroblastoma cells by repressing expression of estrogen receptor alpha (ER-alpha), a nuclear hormone receptor (NHR) (Lovén et al., 2010). Furthermore, it has been proposed that miRNAs are important in regulating and fine-tuning NHR action at multiple levels (Pandey and Picard, 2010).

NHRs, comprising 48 human (Mangelsdorf et al., 1995) and 49 mouse (Bookout et al., 2006) genes, represent the largest transcription factor superfamily in metazoans. These receptors respond to a wide variety of ligands (Chawla et al., 2001). The majority of NHRs bind DNA either as homo- or heterodimers, and others recruit co-repressors or co-activators in the absence and presence of ligand, respectively (Tata, 2002). NHRs play an important role in controlling the fate of neural stem cells and

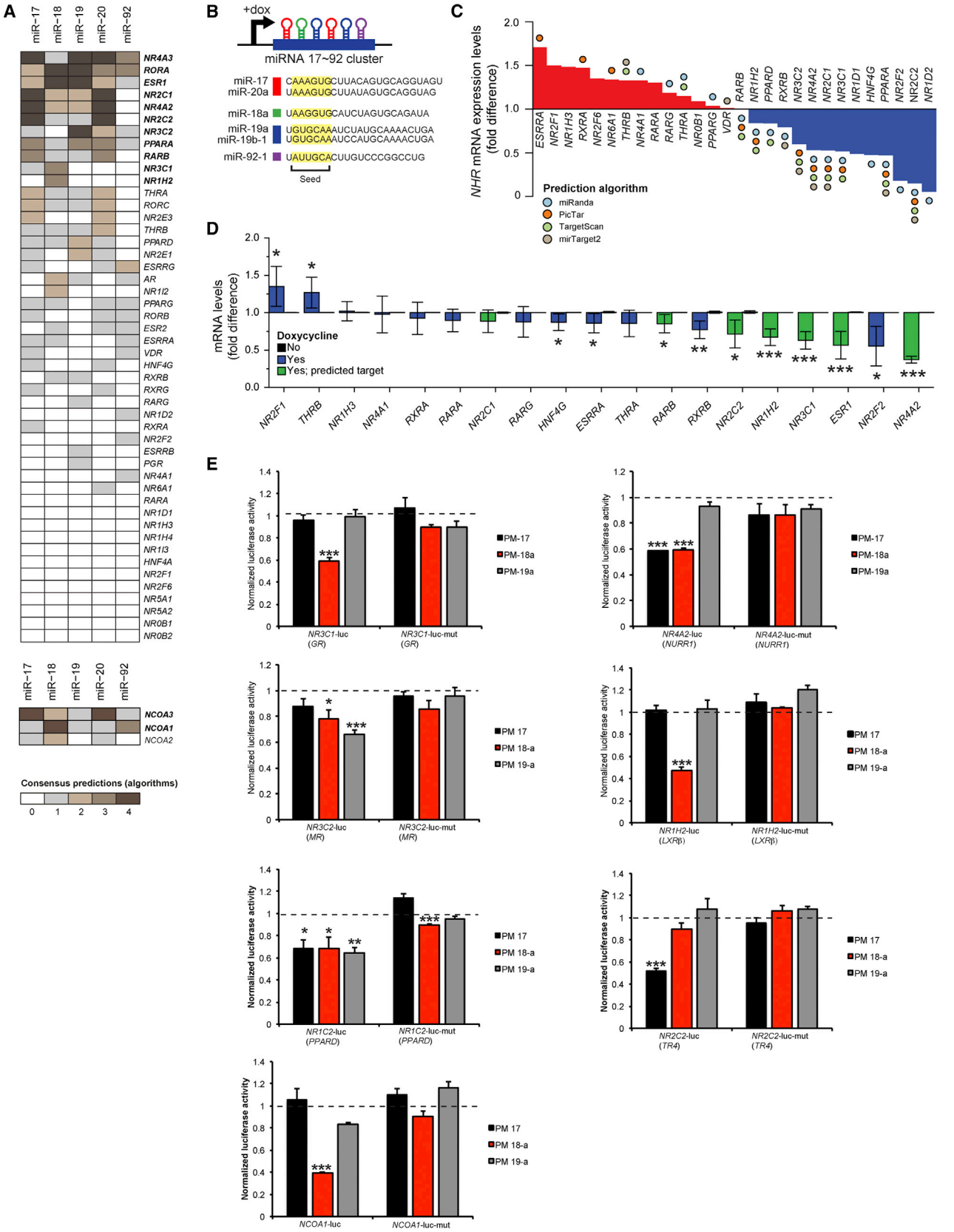

(legend on next page)

neural differentiation (Rada-Iglesias et al., 2012; Stergiopoulos and Politis, 2013). Given that neuroblastoma arises from the developing neural crest, we hypothesized that NHRs might also play important roles in tumorigenesis and progression.

Here, we investigated the role of NHRs in neuroblastoma biology in relation to MYC pathway activity. We found that the expression of several NHR members correlated with increased survival in neuroblastoma patients and with neural differentiation in a MYCN-driven mouse model. Furthermore, we demonstrated that the MYC-regulated miR-17∼92 cluster represses the genes encoding the same NHRs, thereby inhibiting differentiation and contributing to tumorigenesis. Importantly, pharmacological inhibition of MYCN, followed by activation of glucocorticoid signaling, led to a reduced tumor burden in a neuroblastoma mouse model. Our results provide evidence for miR-17∼92-mediated deregulation of NHRs in patients and emphasize a critical role for this transcription factor family in neuroblastoma tumorigenesis.

RESULTS

The miR-17∼92 Cluster Targets the NHR Family

We have previously shown that miR-17∼92 members directly target ER-alpha (*ESR1*) in neuroblastoma as a mechanism to inhibit differentiation (Lovén et al., 2010), and we hypothesized that additional members of the NHR family could be targeted for repression. To identify cognate miR-17∼92 binding sites in the 3′ UTRs of all NHR family members, we used four independent prediction algorithms and selected transcripts predicted by at least three of these algorithms (Figures 1A and S1A; Tables S1, S2, and S3). Of the 48 NHRs, 11 were predicted to contain miR-17∼92 binding sites, representing a disproportional enrichment of sites over the expected distribution ($p = 0.01939$; the Fisher's exact test (Tables S2–S4)). We extended our analysis to the p160 nuclear receptor co-activator (*NCOA*) gene family, whose members act as transcriptional co-activators for a broad range of NHRs (Xu and Li, 2003; Xu et al., 2009), and found that *NCOA1* and *NCOA3* were also consensus-predicted targets (Figure 1A; Table S2).

Next, we sought to confirm our in silico predictions using a neuroblastoma cell line with an inducible miR-17∼92 cluster (Figures 1B and S1B; Mestdagh et al., 2010). Using a low-density array to measure NHR expression levels, we determined that 28 of 48 NHR transcripts were detectable in these cells and that the majority of the downregulated NHRs were predicted targets of miR-17∼92 (8 of 11 consensus NHRs; Figure 1C; Table S3). qPCR analysis confirmed that predicted and previously established NHR targets, including ER-alpha, were downregulated after activation of the miR-17∼92 cluster (Figures 1C and 1D).

We generated reporter plasmids by fusing the 3′ UTRs of several NHRs to the luciferase open reading frame and co-transfected these constructs in HEK293T cells with control pre-miR, pre-miR-17, pre-miR-18a, or pre-miR-19a, three members of the cluster that were previously shown to be important in neuroblastoma tumorigenesis (Fontana et al., 2008; Lovén et al., 2010). We found that miR-17 decreased the luciferase levels of the *NURR1* (also known as *NR4A2*), *PPARD* (*NR1C2*), and *TR4* (*NR2C2*) constructs; whereas miR-18a decreased the luciferase activity of the *LXRβ* (*NR1H2*), *PPARD* (*NR1C2*), *NURR1*, and *GR* (*NR3C1*) reporters; and that miR-19a led to decreased luciferase levels of the *PPARD* and *MR* (*NR3C2*) constructs (Figure 1E). Furthermore, the nuclear receptor co-activator *NCOA1* was validated as a target of miR-18a (Figure 1E). Mutating the respective seed sequences rescued the decreased luciferase levels in all reporter plasmids (Figure 1E). In contrast, no significant changes in luciferase activity were detected in the 3′ UTR-luciferase reporters for *THRA* (*NR1A1*), *THRB* (*NR1A2*), *RARB* (*NR1B2*), *RORA* (*NR1F1*), *TR2* (*NR2C1*), or *NOR1* (*NR4A3*) (Figure S1C). Importantly, we identified *GR*, *NURR1*, *MR*, *LXRβ*, *PPARD*, *TR4*, and *NCOA1* as direct targets of the miR-17∼92 cluster.

An NHR Signature Is Associated with Overall Neuroblastoma Patient Survival

To evaluate the clinical relevance of NHRs in neuroblastoma, we used a cohort of 649 untreated patients in all stages of disease (Kocak et al., 2013) and searched for NHRs differently expressed in *MYCN*-amplified versus non-*MYCN*-amplified cases. Six of the eleven consensus-predicted NHRs (*NR3C1*, *NR3C2*, *NR4A2*, *RORA*, *NR4A3*, and *ESR1*) and the co-activator *NCOA1* were significantly downregulated in *MYCN*-amplified patients (Figure 2A; Table S5). Importantly, at least five of these seven genes are direct targets of miR-17∼92 (Figure 1E), with *GR* (*NR3C1*) and *NURR1* (*NR4A2*) ranking among the top downregulated transcripts in *MYCN*-amplified neuroblastoma (Figure 2A). By using these seven transcripts, we generated an "NHR score" (Table S6). Considering that both MYCN and MYC can activate the miR-17∼92 cluster (Lovén et al., 2010;

Figure 1. Several NHRs Are Putative Targets of the miR-17∼92 Cluster

(A) Heatmaps depicting members of the nuclear hormone receptor (NHR) and nuclear receptor co-activator (NCOA) families as targets of the miR-17∼92 cluster. Gene names are shown to the right and the miR-17∼92 members (miR-17, miR-18, miR-19, miR-20, and miR-92) on top of the heatmaps. The key to the number of consensus algorithms that predict seed sequences for the different miRNAs is shown below the heatmaps. The 11 NHR and the two NCOA genes with the highest consensus are presented in bold face.

(B) A schematic of the miR-17∼92 cluster (top) and their "seed region" sequences (bottom). In SHEP-TR-miR-17∼92 cells, the miR-17∼92 cluster is expressed from a doxycycline (dox)-inducible promoter in the SHEP neuroblastoma cell line.

(C) A histogram showing differential mRNA expression of NHRs in SHEP-TR-miR-17∼92 cells, with high versus low miR-17∼92 expression. Red and blue indicate increased and decreased NHR gene expression levels, respectively. The circles represent algorithms predicting a particular gene as a target for the cluster.

(D) Validation of identified NHR targets using qRT-PCR. Bars of consensus-predicted targets are colored green. $n = 5$; the mean ± SEM is shown for quantitation; $^{*}p < 0.05$; $^{**}p < 0.01$; and $^{***}p < 0.001$, compared to the activity of the uninduced miR-17∼92 cluster.

(E) Luciferase assays of the indicated NHR 3′ UTR-luciferase constructs co-transfected into HEK293T cells with pre-miR-scrambled, pre-miR-17 (PM-17), pre-miR-18a (PM-18a), or pre-miR-19a (PM-19a). The dotted line indicates the luciferase activity following transfection with pre-miR-scrambled plasmid. Luciferase activity was also assessed using 3′ UTR-NHR reporters with mutated seed sequences as indicated. Experiments were performed at least four times with the mean ± SEM; $^{*}p < 0.05$; $^{**}p < 0.01$; and $^{***}p < 0.001$, compared to the luciferase activity of the pre-miR-scrambled plasmid.

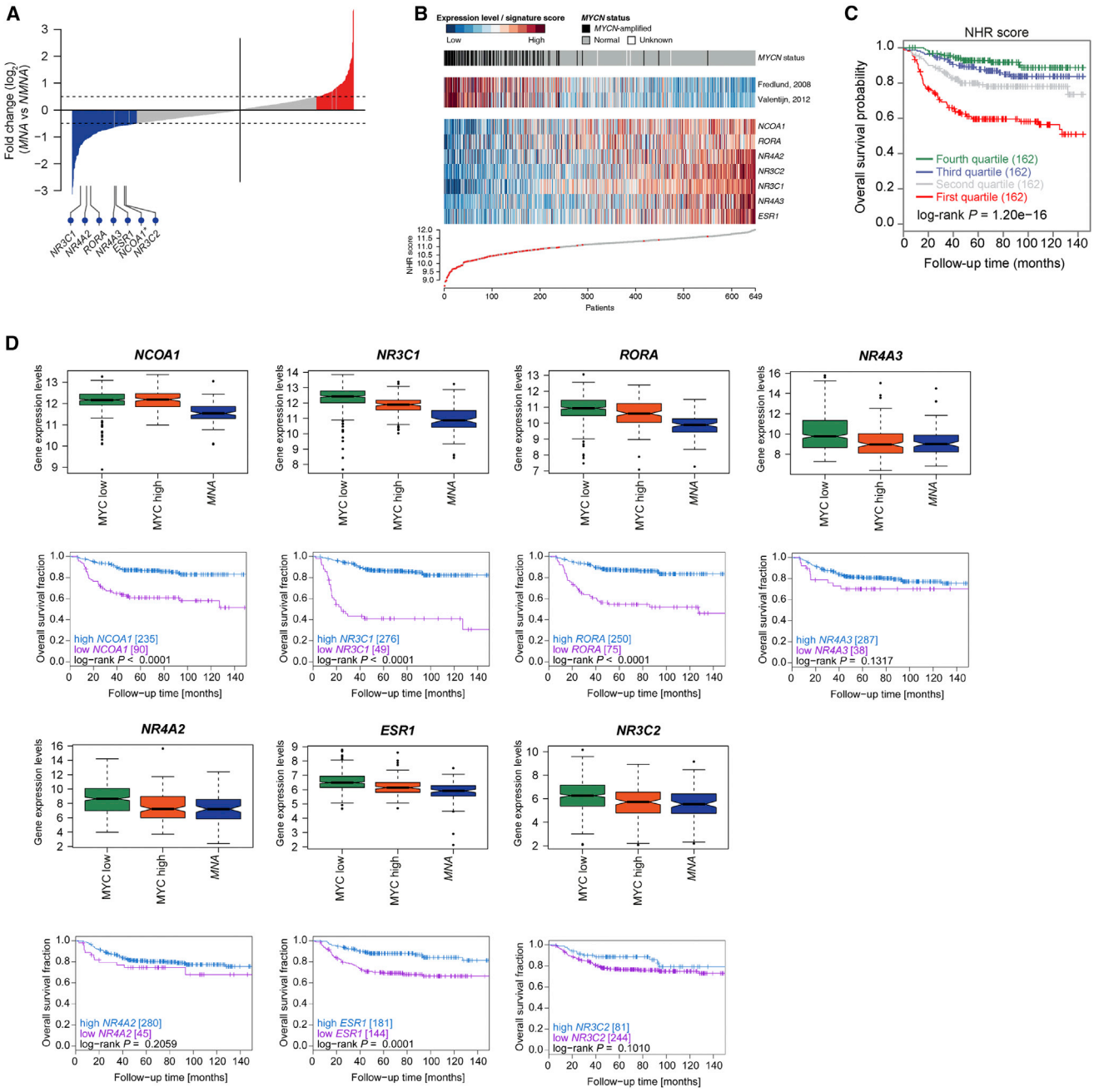

Figure 2. The NHR Score Is Associated with Survival in Neuroblastoma Patients

(A) Differentially expressed genes in *MYCN*-amplified versus non-*MYCN*-amplified neuroblastoma in a cohort of 649 untreated patients. Significantly differential gene expression is marked by the dashed lines ($q < 0.05$ and $\log_2$-difference > 0.5). The positions of the predicted NHRs targets of miR-17∼92 are marked below the graph.

(B) An "NHR score" was generated based on seven consensus-predicted NHRs or NHR-related targets (*NCOA1*, *RORA*, *NR4A2*, *NR3C2*, *NR3C1*, *NR4A3*, and *ESR1*) and then sorted according to the expression levels represented in the histogram below the heatmaps. Gene expression data from 649 neuroblastoma patients were sorted and correlated to *MYCN* amplification, MYC signature, and expression levels of the individual NHRs represented in the NHR score. Red indicates high expression whereas blue represents low expression levels. *MYCN* status is presented as amplified, normal gene copy number, or unknown.

(C) Neuroblastoma patients (n = 649) categorized into four equal-size quartile groups based on their NHR score. The first quartile (red) represents patients with the lowest NHR score, and the fourth quartile (green) represents those with the highest NHR score. Statistical analyses were performed comparing the first quartile to the other three (p = 1.20e–16).

(legend continued on next page)

O'Donnell et al., 2005; Schulte et al., 2008), we first scored the patients according to their inferred MYC signaling status (Fredlund et al., 2008; Valentijn et al., 2012) and then sorted the patients according to their NHR scores (Figures 2B and S2A; Table S6; Supplemental Information). There was a strong inverse relationship between the NHR score and *MYCN* amplification and/or MYC signaling (both signatures $p < 0.001$; Figure S2A). Patients with active MYC signaling showed low expression levels of the predicted NHR family members and vice versa (Figure 2B), suggesting an inverse correlation between NHR expression and MYC signaling in neuroblastoma (Figure 2B; Table S6). Importantly, patients with the lowest NHR score (first quartile; Figure 2C) had significantly worse survival compared to patients with higher NHR scores (second, third, and fourth quartiles; Figure 2C).

Next, we investigated the impact of all NHR family members on overall survival. Approximately half of the 42 available transcripts were associated with patient outcome. These included genes encoding the retinoic acid and steroid hormone receptors, such as the glucocorticoid receptor (GR) and the orphan receptor NURR1 (Table S7). The expression of nearly all NHR score members, including GR, was low in *MYCN*-amplified tumors, and reduced expression was associated with poor overall survival in patients (Figures 2D and S2B). Together, these data show that several NHRs targeted by miR-17∼92 are downregulated in MYCN-driven neuroblastoma and correlate with survival.

MYCN-Mediated Downregulation of GR Is Associated with Neuroblastoma Tumorigenesis

To further analyze the significance of NHRs in neuroblastoma, we focused on the GR (*NR3C1*) because it is (1) a direct target of the miR-17∼92 cluster (Figure 1E; Vreugdenhil et al., 2009), (2) the most significantly downregulated NHR in *MYCN*-amplified patients (Figure 2A; Table S5), and (3) highly prognostic for patient outcome (Figure 2D). Additionally, GR is expressed in the sympathetic nervous system, particularly in the adrenal gland (Bohn et al., 1984; Parlato et al., 2009), a site where neuroblastoma typically arises (Maris, 2010).

We first investigated the impact of MYCN or miR-17∼92 on GR protein expression in three different neuroblastoma cell lines, with inducible expression of MYCN (MYCN3 and Tet-21/N; Lutz et al., 1996; Slack et al., 2005) or miR-17∼92 (SHEP-TR-miR-17∼92; Mestdagh et al., 2010). Endogenous GR levels decreased 2-fold in the presence of either MYCN or miR-17∼92 (Figure 3A). Accordingly, GR expression was reduced in MYCN-induced cells as analyzed by immunofluorescence (Figure 3B).

Next, we analyzed the levels of GR in the postnatal sympathetic ganglia in wild-type and homozygous *TH-MYCN* mice, a transgenic model of neuroblastoma where *MYCN* is overexpressed in the neural crest (Rasmuson et al., 2012; Weiss et al., 1997). The sympathetic identity of the GR-expressing cells was confirmed by co-staining for tyrosine hydroxylase (TH) (Cochard et al., 1978). We detected robust nuclear GR levels and TH expression at postnatal day 24 (P24) in the cervical, thoracic, and lumbar sympathetic ganglia (Figure 3C) and in the adrenal medulla (Figure 3D) of wild-type mice.

As previously described (Hansford et al., 2004), analysis of homozygous *TH-MYCN* mice revealed the presence of hyperplastic lesions characterized by clusters of small round cells within the sympathetic ganglia, which were not detected in wild-type mice (Figures 3C and 3E). These hyperplasias expressed high MYCN levels but no detectable expression of the neuronal differentiation markers TH or TrkA (Figures 3E and 4A), indicating an undifferentiated state. Conversely, mature TH- and TrkA-positive neuronal cells in wild-type and homozygous mice were MYCN-negative (Figures 3E and 4A). We did not detect GR in MYCN-positive hyperplasias, whereas GR expression was present in the MYCN-negative normal surrounding ganglionic tissue and wild-type adrenal medulla (Figures 3D and 3E). Furthermore, an inverse relationship between *Mycn* and *Nr3c1* mRNA was also observed in neural crest cells at embryonic day (E) 8.5 and E13.5 as well as in the adrenal medulla at P90 in CD-1 mice (Figures 3F and 3G; Albino et al., 2011) and in sympathetic tissue in *TH-MYCN* mice (Figure 3H; Heukamp et al., 2012).

We detected tumors expressing high levels of MYCN in the lumbar region as early as P24 (Figure S3A). Similar to the hyperplasias, GR expression was low or absent in P24 and adult tumor cells (Figures S3A and S3B). Numerous scattered GR-positive cells were present within the tumors, which were associated with the vasculature as assessed by co-staining for the endothelial marker endomucin (Figure S3C). These results show that deregulation of GR in hyperplastic tissues is maintained during the late stages of tumor development. We confirmed previous studies demonstrating that miR-17∼92 and especially miR-18a are highly expressed in *TH-MYCN* tumors compared to normal adrenal tissue (Figure S3D; Terrile et al., 2011). Furthermore, expression data from *TH-MYCN* tumors revealed an inverse relationship between *Nr3c1* mRNA expression and tumor mass ($R^2 = -0.67$; Figure 3I). *Nr3c1* expression was positively associated with overall survival in these mice (Figure S3E; Balamuth et al., 2010), as well as in neuroblastoma patients (Figure 2D; Table S7).

Together, these results show that GR is downregulated by MYCN through miR-17∼92 both in vitro and in vivo and that its expression correlates both with an undifferentiated phenotype and with decreased survival in neuroblastoma patients as well as in *TH-MYCN* mice.

Glucocorticoid Signaling Influences the Differentiation of Neuroblastoma

It has been suggested that the GR may regulate neuronal gene expression in the sympathoadrenal lineage (Polman et al., 2012). Similar to TH and GR, TrkA was readily detected in normal

(D) (Upper panels) Expression levels of the NHR score transcripts comparing neuroblastoma patients with low-MYC signaling (MYC low), high-MYC signaling (MYC high), and *MYCN*-amplified (*MNA*) tumors (n = 649; 278 patients in both the MYC-low and -high groups and 93 *MNA* patients). (Lower panels) Overall survival of neuroblastoma patients in the validation cohort (n = 325) according to the prognostic expression cutoff value determined for each of the seven NHR score genes in the training cohort (n = 324) is shown. Patient numbers are indicated in brackets.

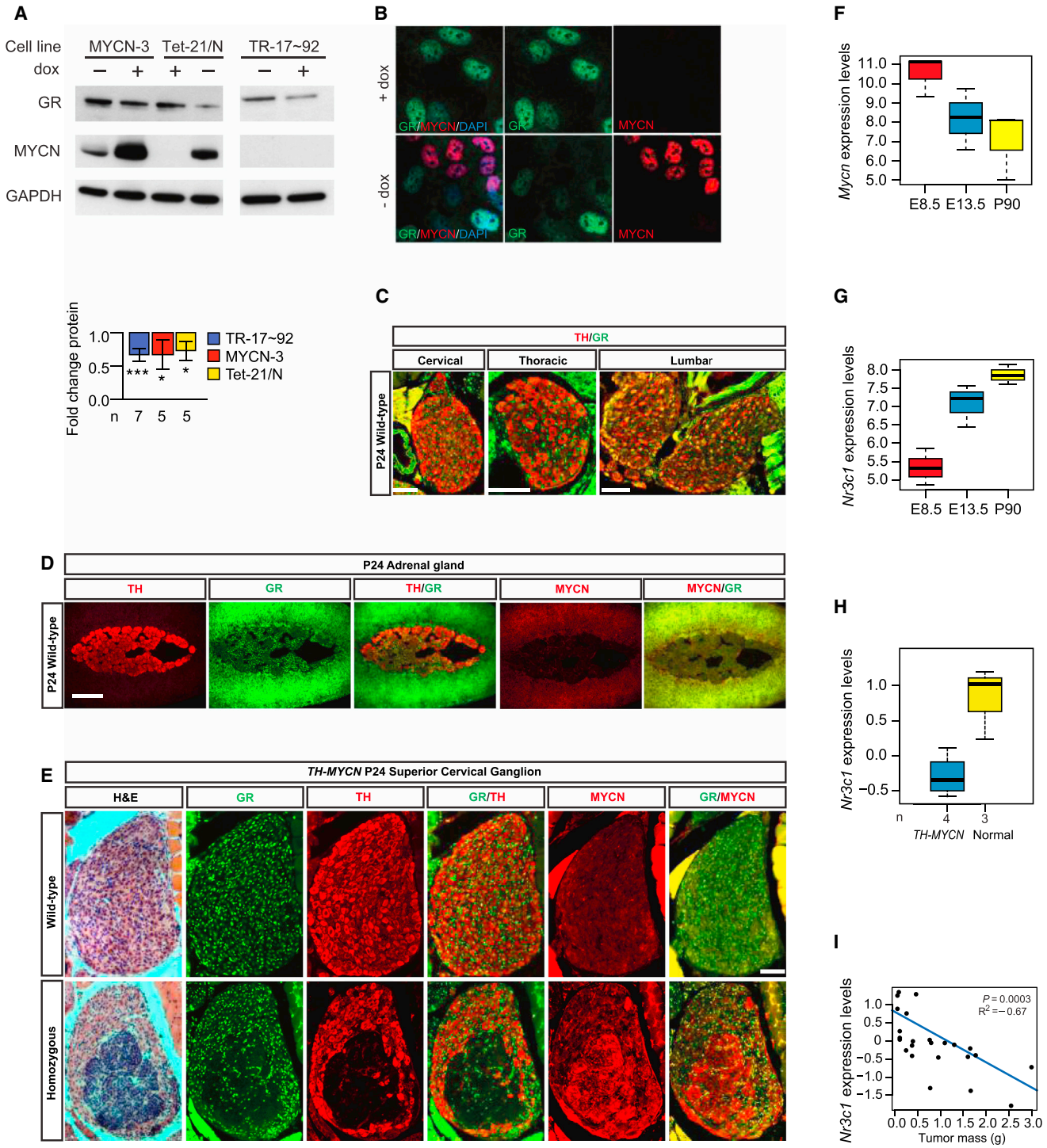

Figure 3. Both miR17∼92 and MYCN Inhibit GR Activity In Vitro and In Vivo

(A) Immunoblotting of GR and MYCN in MYCN3, Tet-21/N, and SHEP-TR-miR-17∼92 (TR-17∼92). Cells were treated with dox for 48 hr. Experiments were performed at least five times, with the mean ± SEM reported for quantification; *p < 0.05; **p < 0.01; and ***p < 0.001, compared to either miR-17∼92-high or MYCN-high states. GAPDH was used as loading control.

(B) Immunofluorescence of GR and MYCN in Tet-21/N cells treated with or without dox for 48 hr. One representative out of three independent experiments is shown.

(C) Immunohistochemistry for GR and TH at P24 in the sympathetic ganglia from three anatomic levels (cervical, thoracic, and lumbar). The scale bar represents 100 μm.

(D) GR expression in the adrenal medullary cells from wild-type mice, as assessed by co-expression with TH. The scale bar represents 200 μm.

(legend continued on next page)

neuronal tissue, but not in MYCN-positive hyperplastic areas or in tumors from *TH-MYCN* mice (Figures 4A and S4A), further strengthening the notion that a deficit in GR expression is associated with a more immature and undifferentiated phenotype. *TRKA* expression has been inversely correlated to *MYCN* amplification and is a well-known marker of favorable outcome in neuroblastoma (Brodeur et al., 1997; Kogner et al., 1993), as also observed in our patient cohort (Figures 4C and 4D).

To determine whether GR can directly influence neural differentiation, we used a *MYCN*-amplified neuroblastoma cell line, SK-N-BE(2), stably expressing either an anti-miR-18a or a scrambled control. As previously shown, BE(2)-anti-miR-18a cells displayed a more-differentiated phenotype compared to control cells (Figure S4B; Lovén et al., 2010). *GR* expression was significantly higher in miR-18a knockdown cells compared to control cells (Figure 4G). In agreement with a well-described negative feedback loop (Kalinyak et al., 1987), hydrocortisone (HC) treatment induced a decrease in *GR* mRNA levels in BE(2)-anti-miR18a cells (Figure 4G). In addition, neurite outgrowth and *TRKA* levels increased significantly following incubation with HC (Figures S4B and 4H), indicating that activation of GR signaling in miR18a-depleted cells induces neural differentiation.

We further analyzed a known GR target, secretogranin II (SCG2) (Finotto et al., 1999; Polman et al., 2012). This neuroendocrine protein is implicated in the packaging and sorting of hormone peptides and neurotransmitters into secretory vesicles (Ozawa and Takata, 1995) and expressed in the adrenal gland (Figure S4C; Steiner et al., 1989). However, *Scg2* is completely absent from adrenal medullary cells in *Gr*-null mice (Finotto et al., 1999), indicating that GR is required for its expression in adrenal tissues. Importantly, SCG2 is involved in the differentiation of neuroblastoma cells in vitro (Cozzi et al., 1989; Li et al., 2008).

We detected SCG2 in cell bodies and fibers in the sympathetic ganglia of wild-type mice (Figure 4B) as well as in TH-expressing cells of the adrenal medulla (Figure S4C; Steiner et al., 1989). Similar to GR, TH, and TrkA, SCG2 was absent in MYCN-positive hyperplasias and tumors in homozygous *TH-MYCN* mice (Figures 4B and S4D). Accordingly, *SCG2* was downregulated in neuroblastoma tumors with *MYCN* amplification or with high-MYC signaling (Figure 4E), and its expression was highly prognostic (Figure 4F). Moreover, the expression of *SCG2* was increased by 2-fold when miR-18a was knocked down in *MYCN*-amplified neuroblastoma cells (Figure 4I), and treatment with HC further increased mRNA levels, confirming that GR signaling induces *SCG2* expression also in BE(2)-miR-18a cells (Figure 4I). Together, our data demonstrate that GR signaling is increased upon miR-18a depletion and promotes a differentiated phenotype whereas reduced GR levels correlate with low TrkA and SCG2 expression and an undifferentiated state.

Disruption of MYC Signaling Increases GR Expression

Next, we evaluated the effect of disruption of MYC signaling on GR expression in vivo. Hemizygous *TH-MYCN* mice were treated for 6 days with vehicle or 10058-F4, a small MYC-binding molecule that prevents MYC-MAX interaction (Müller et al., 2014; Yin et al., 2003; Zirath et al., 2013). Treatment with 10058-F4 increased the number of GR-positive cells by 50% compared to the vehicle-treated tumors (Figures S5A and S5C). Most GR-positive cells detected in vehicle-treated hemizygous tumors were endothelial cells (Figure S5B). Despite some overlap between GR and MYCN, GR-positive cells were generally negative for MYCN (Figure S5A; high magnification). These results indicate that disruption of MYC signaling increases the number of GR-positive tumor cells in vivo. Furthermore, GR-expressing cells not associated with the vasculature were positive for TH, indicating a more-differentiated phenotype (Figure S5D).

Pharmacological Inhibition of MYCN followed by Activation of GR Signaling Promotes Differentiation and Reduces Tumor Burden

Next, we addressed the functional role of GR signaling in neuroblastoma biology. SK-N-BE(2) cells were treated for 6 days with dexamethasone (DEX), a synthetic ligand of GR, and with 10058-F4, alone and in combination where DEX was added after 72 hr of pre-treatment with 10058-F4 (10058-F4+DEX; Figures S6A and 5A–5G). We found that expression of miR-17, miR-18a, and miR-19a was decreased by all treatments, with the most-robust effect in the 10058-F4+DEX combination (Figure S6B). Treatment with 10058-F4 reduced MYCN levels (Figures 5A and 5D; Zirath et al., 2013), whereas GR expression was upregulated, which is consistent with an inverse relationship between MYCN and GR (Figures 5A and 5E). Whereas no changes in MYCN were observed with DEX treatment alone, the 10058-F4-induced reduction of MYCN was further decreased in the combination treatment (10058-F4+DEX; Figures 5A and 5D). As expected, DEX, alone or with 10058-F4, promoted a decrease in GR levels (Figures 5A and 5E; Kalinyak et al., 1987). The effects on GR and MYCN expression were confirmed using two other MYC inhibitors, 10074-G5 and JQ1, separately and in combination with DEX as well as by incubating the *MYCN*-amplified KCN69n cell line with 10058-F4 and DEX alone and in co-treatment (Figures S6C and S6D).

To evaluate the impact of activation of GR signaling in *MYCN*-amplified neuroblastoma, we assessed the expression of poly (ADP-ribose) polymerase (PARP), proliferating cell nuclear antigen (PCNA), and TrkA, markers for apoptosis, cell proliferation, and differentiation, respectively. Whereas full-length PARP was detected in all conditions, cleaved PARP was only present following treatment with 10058-F4 and increased when 10058-F4 was combined with DEX (Figure 5B). In contrast, PCNA levels were reduced following 10058-F4 incubation and were further

(E) H&E stain and immunohistochemistry for TH, GR, and MYCN in adjacent sections of the superior cervical ganglia in age-matched wild-type and homozygous P24 *TH-MYCN* mice. Three wild-type and four transgenic mice were analyzed. The scale bar represents 100 μm.
(F) *Mycn* mRNA expression during normal development (E8.5, E13.5, and P90) in wild-type mice (Albino et al., 2011).
(G) *Nr3c1* mRNA expression during normal development (E8.5, E13.5, and P90) in wild-type mice (Albino et al., 2011).
(H) mRNA expression levels of *Nr3c1* in *TH-MYCN*-derived ganglia compared to wild-type adrenal tissue (normal; Heukamp et al., 2012).
(I) Correlation between *Nr3c1* mRNA expression and tumor mass in *TH-MYCN* mice ($p < 0.001$; $R^2 = -0.67$; Balamuth et al., 2010).

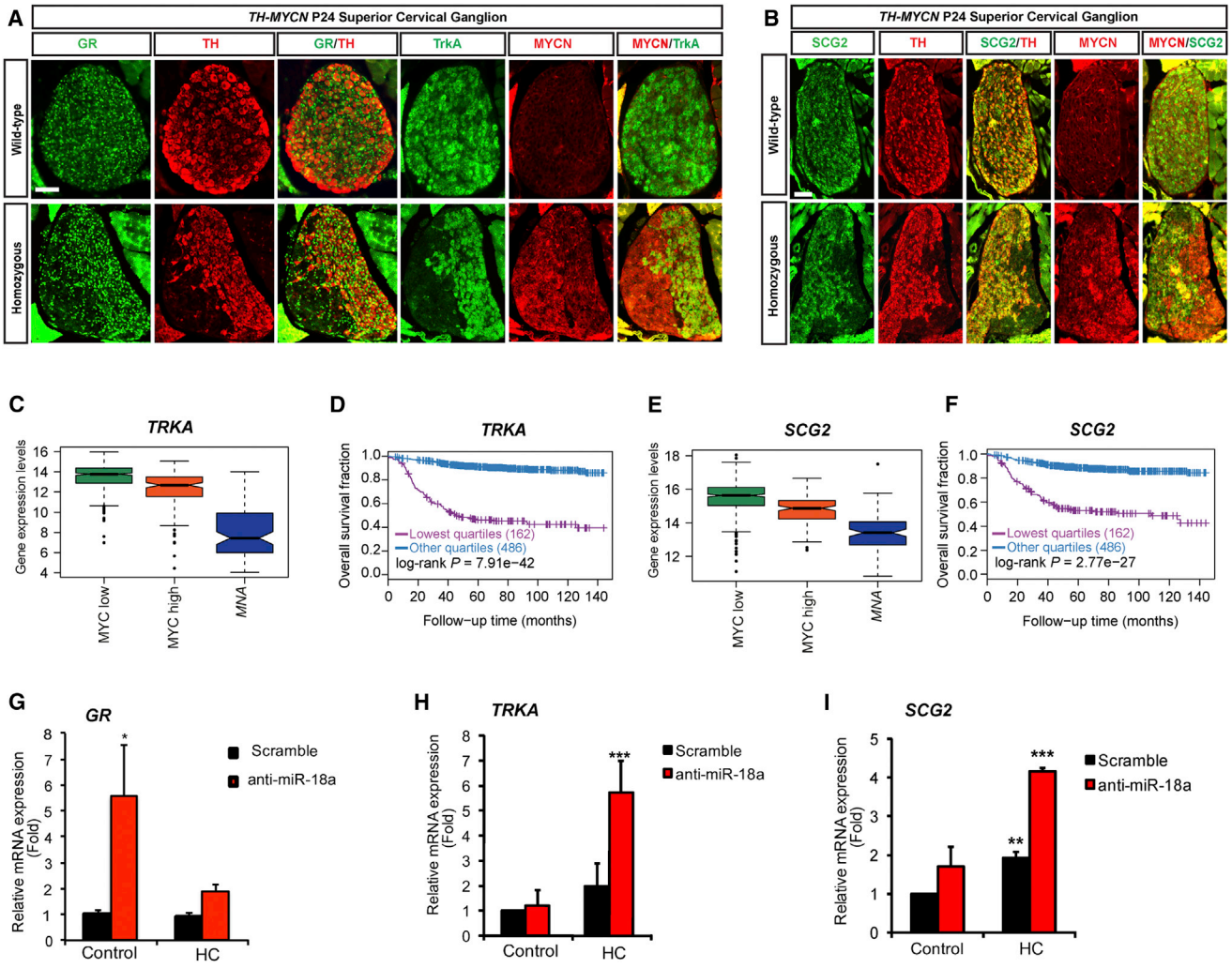

Figure 4. GR Expression and Signaling Correlate to Increased Expression of Differentiation Markers Both In Vitro and In Vivo

(A) Immunohistochemistry for TH, GR, and TrkA in adjacent sections of the superior cervical ganglia in wild-type and homozygous P24 *TH-MYCN* mice. The scale bar represents 100 μm.

(B) Immunohistochemistry for TH, SCG2, and MYCN in adjacent sections of the superior cervical ganglia in age-matched wild-type and homozygous P24 mice. The scale bar represents 100 μm.

(C) Expression levels of *TRKA* comparing neuroblastoma patients with low-MYC signaling (MYC low), high-MYC signaling (MYC high), and *MYCN*-amplified (*MNA*) tumors (n = 649, 278 patients in both the MYC-low and -high groups and 93 *MNA* patients).

(D) A Kaplan-Meier plot based on *TRKA* mRNA expression levels correlated to overall survival. Neuroblastoma patients (n = 649) categorized into four equally sized quartile groups based on *TRKA* expression are shown. The quartile with the lowest expression is shown in purple ($p < 0.001$).

(E) Expression levels of *SCG2* comparing neuroblastoma patients with low-MYC signaling (MYC low), high-MYC signaling (MYC high), and *MYCN*-amplified (*MNA*) tumors (n = 649, 278 patients in both the MYC-low and -high groups and 93 *MNA* patients).

(F) A Kaplan-Meier plot based on the *SCG2* mRNA expression levels correlated to overall survival. Neuroblastoma patients (n = 649) were categorized into four equally sized quartile groups based on *SCG2* expression levels. The quartile with the lowest expression is shown in purple ($p < 0.001$).

(G) qPCR analysis of *NR3C1* (*GR*) expression in SK-N-BE(2) cells transduced with either a scrambled-miRNA (scramble) or an anti-miR-18a (anti-miR-18a) lentivirus and treated with and without the natural ligand hydrocortisone (HC). n = 5 (*$p < 0.05$).

(H) qPCR analysis of *TRKA* expression in SK-N-BE(2) cells transduced with either a scrambled-miRNA (scramble) or an anti-miR-18a (anti-miR-18a) lentivirus and treated with and without hydrocortisone (HC). n = 5 (***$p < 0.001$).

(I) qPCR analysis of *SCG2* expression in SK-N-BE(2) cells transduced with either a scrambled-miRNA (scramble) or an anti-miR-18a (anti-miR-18a) lentivirus treated with and without hydrocortisone (HC). n = 5 (**$p < 0.01$; ***$p < 0.001$).

decreased upon DEX addition (Figure 5C). We found that DEX moderately increased TrkA whereas 10058-F4 led to a more-robust TrkA expression, both alone and in combination with DEX (Figures 5F and 5G).

Next, we analyzed the role of GR in differentiation in cells derived from the *TH-MYCN* mouse model. Tumor cells were isolated and grown as spheres that differentiated into TH-positive sympathetic neurons under differentiation conditions (Figure 5H).

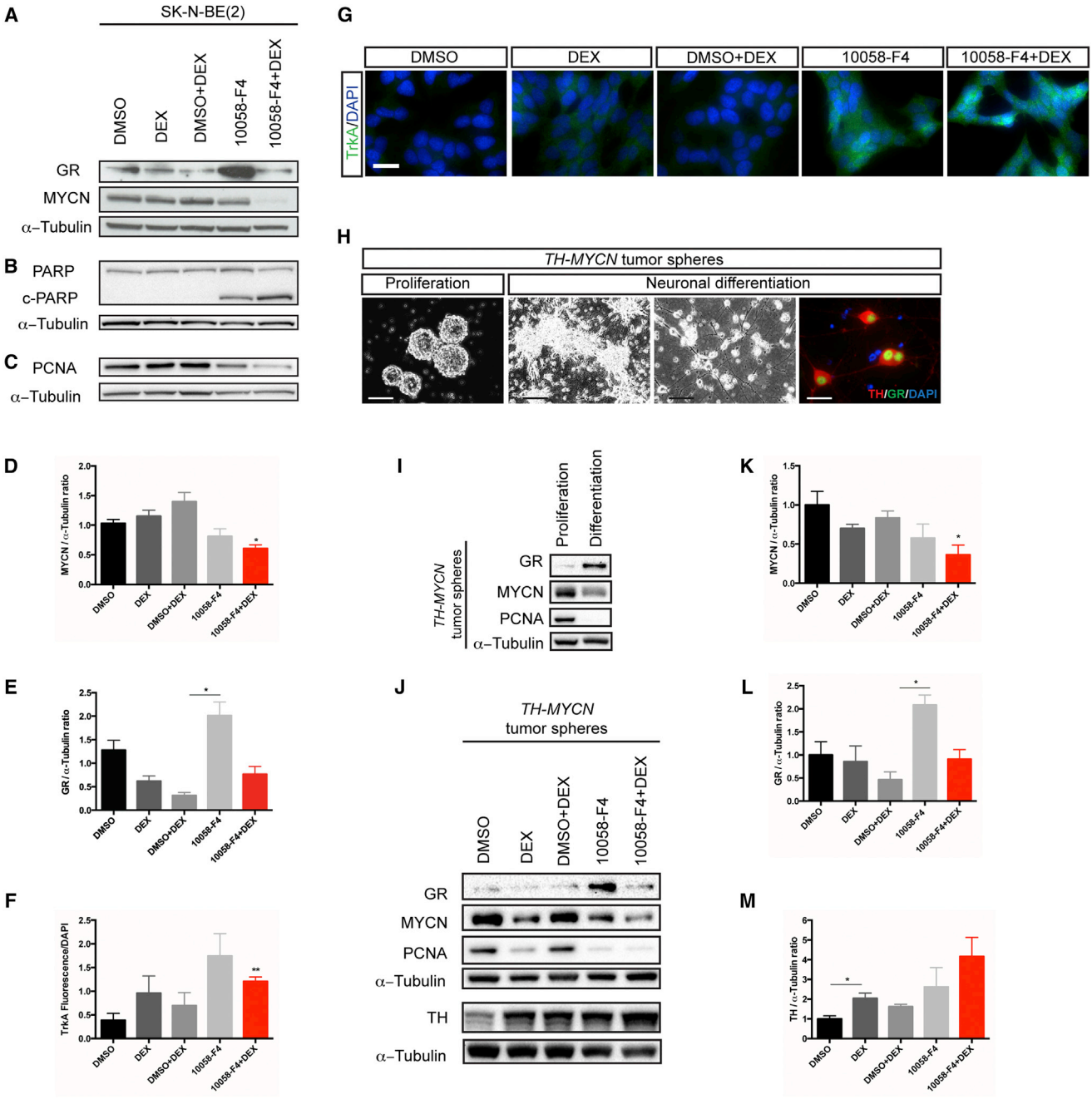

Figure 5. Inhibition of MYCN followed by Activation of GR Signaling Promotes Neural Differentiation

(A–C) Immunoblotting of GR and MYCN (A), PARP (B), and PCNA (C) in the SK-N-BE(2) cell line. Cells were incubated for 6 days with DEX and/or 10058-F4, alone and in combination, where DEX and 10058-F4 were added after 72 hr of pre-treatment with 10058-F4 (10058-F4+DEX). Control cells were treated with DMSO, DEX, or both in combination after DMSO pre-incubation (DMSO+DEX). See Figure S6A for experimental scheme. Representative blots from five experiments are shown. α-tubulin was used as a loading control.

(D and E) Quantification of MYCN (D) and GR (E) by densitometry. n = 5 with the mean ± SEM shown for quantification; *$p < 0.05$ compared to DMSO-treated cells.

(F) Quantification of TrkA immunofluorescence in treated SK-N-BE(2) cells. n = 5 with the mean ± SEM shown for quantification; **$p < 0.01$ compared to DMSO-treated cells.

(G) Immunofluorescence of TrkA in treated SK-N-BE(2) cells. One representative out of five independent experiments is shown. The scale bar represents 25 μm.

(H) Proliferation and differentiation of *TH-MYCN* spheres. Bright field microscopy pictures in two different magnifications of tumor spheres in proliferation or differentiation conditions as indicated are shown. Immunofluorescence of TH (red) and GR (green) is shown. DAPI (blue) stains the DNA. The scale bars represent 25 μm.

(legend continued on next page)

Notably, when proliferating spheres were induced to differentiate, GR expression was upregulated with a concomitant reduction in MYCN levels (Figure 5I). In addition, we observed that the majority of neurons co-expressed GR and TH (Figure 5H). We employed our scheme with 10058-F4 and DEX (Figure S6A) on the *TH-MYCN*-derived tumor spheres. As expected, 10058-F4 induced a decrease in MYCN levels with a concomitant upregulation in GR (Figures 5J–5L). DEX also promoted a reduction in MYCN levels, and the combination treatment with 10058-F4 potentiated this decrease (Figures 5J and 5K). Importantly, both DEX and 10058-F4 stimulated an increase in TH expression, which was further enhanced when both compounds were used together (Figures 5J and 5M). As in SK-N-BE(2) cells, all treatments resulted in a reduced expression of miR-17, miR-18a, and miR19a, particularly the combination treatment (Figure S6E).

To further clarify the role of GR in neuroblastoma differentiation, we generated SK-N-BE(2) neuroblastoma cells stably expressing GR using a cumate-inducible lenti-vector. As control, cells were transduced in parallel with an empty vector. Whereas GR was low or undetectable in the control BE(2)-EV cells, we observed GR expression in the BE(2)-*GR* cells even in the absence of cumate, indicating certain leaky gene expression (Figures 6A, 6B, S6F, and S6G). However, cumate promoted a robust dose-dependent induction of GR followed by a modest reduction in MYCN levels (Figures S6F–S6H). Importantly, GR overexpression stimulated TH levels, which were further increased by DEX treatment (Figures 6B and 6C).

Together, our data reveal that activation of GR signaling following MYCN inhibition promotes neuronal differentiation, while reducing cell proliferation and stimulating apoptosis. Similarly, GR overexpression in *MYCN*-amplified neuroblastoma cells stimulates neural differentiation, which in turn is potentiated by DEX treatment, further supporting a role for GR signaling in promoting neural differentiation (Figures 6B and 6C).

To evaluate the therapeutic potential of activation of GR signaling in *MYCN*-amplified neuroblastoma, we performed xenotransplantation experiments in which nude mice were injected subcutaneously with SK-N-BE(2) cells followed by treatment with 10058-F4 and DEX alone and in combination (Figure S7A). By day 5, we observed a significant decrease in both tumor volume and in tumor volume index in all treated animals compared to vehicle-treated mice (Figures 6D and S7B). Importantly, at the endpoint, this decline was only maintained in the DEX10 and 10058-F4+DEX10 groups, with a stronger effect in the latter (Figure 6D). These results were corroborated by analysis of tumor weight (Figure 6E). In agreement with the in vitro experiments, a robust decrease in MYCN levels was only detected in the combination treatment, whereas no significant changes were detected in tumors from other treatment groups (Figures 6F, 6G, and S7C). In conclusion, our results reveal MYCN inhibition followed by activation of glucocorticoid signaling as a potential new combination therapy for treating high-risk, *MYCN*-amplified neuroblastoma patients.

DISCUSSION

Both *MYCN* amplification (Brodeur, 2003) and MYC signaling (Fredlund et al., 2008; Valentijn et al., 2012) correlate with aggressive tumor growth and poor prognosis in neuroblastoma. Our study identifies several members of the NHR superfamily as targets of the miR-17∼92 cluster and shows that NHR expression correlates to survival in neuroblastoma patients. Seven putative miR-17∼92 NHR targets (NHR score) were significantly inversely correlated with *MYCN* amplification and MYC pathway activity. Importantly, a high NHR score and expression of individual NHRs were significantly associated with increased survival, indicating an important role for NHRs in neuroblastoma biology.

We also found that the co-activator NCOA1, which enhances the activity of several NHRs (Onate et al., 1998), is regulated by the miR-17∼92 cluster, supporting widespread control of NHR activity by this miRNA family. Given the neural origin of neuroblastoma, it is important to note that many of these NHRs play essential roles in neural development (e.g., NURR1 and liver X receptors; Sacchetti et al., 2009; Zetterström et al., 1997) and in the differentiation of neurons (e.g., mineralocorticoid receptor; Munier et al., 2010).

The GR has been implicated in several neural development processes, including cell proliferation, brain growth, and remodeling of axons and dendrites (Meyer, 1983, 1985). In the sympathetic nervous system, GR is expressed in the ganglia (Bohn et al., 1984) and in medullary adrenal chromaffin cells, where it promotes expression of catecholaminergic characteristics (Smith and Fauquet, 1984). Given that neurohormone expression is linked with differentiation, these studies underline the importance of glucocorticoid signaling in neuronal maturation. We only detected nuclear GR in the sympathetic ganglia during the postnatal stages, further strengthening the concept that GR expression is associated with (or a property of) terminally differentiated sympathetic neuronal cells.

MYCN plays a crucial role in the migration of neural crest cells during development but is turned off in mature neural cells (Zimmerman et al., 1986). Interestingly, *Gr* expression is low during mouse embryonic development of sympathetic ganglia, whereas *Mycn* expression is high; however, this relationship becomes inverted after birth. We suggest that persistent high MYCN levels may contribute to neuroblastoma development by repressing several NHRs through miR-17∼92, thereby rendering the cells unresponsive to hormones and other ligands required for final neuronal differentiation (Figure 7). Our data

(I) Immunoblotting of GR, MYCN, and PCNA during proliferation and differentiation of *TH-MYCN* spheres. Representative blots from five experiments are shown. α-tubulin was used as loading control.

(J) Immunoblotting of GR and MYCN, PCNA, and TH in spheres from the *TH-MYCN* tumors. Spheres were treated for 6 days with DEX or 10058-F4 separately and in a combination, where DEX and 10058-F4 were added together after 72 hr of pre-treatment with 10058-F4 (Figure S6A). Control cells were treated with DMSO or DEX alone and in combination (DMSO+DEX). Representative blots from five experiments are shown. α-tubulin was used as loading control.

(K–M) Quantification of MYCN (K), GR (L), and TH (M) by densitometry. n = 5 with the mean ± SEM shown for quantification; *$p < 0.05$ compared to DMSO-treated for MYCN and TH and compared to DMSO+DEX for GR.

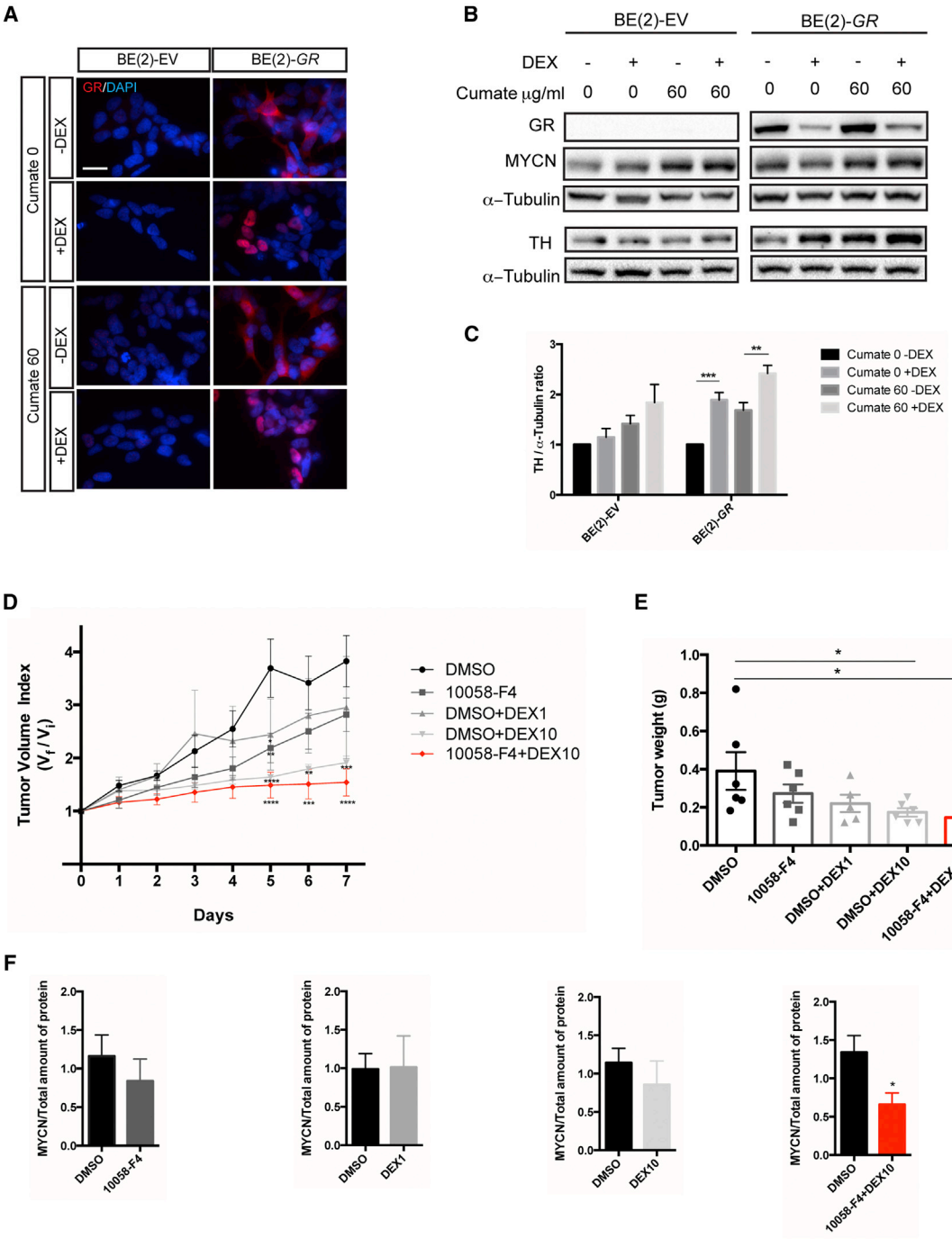

(legend on next page)

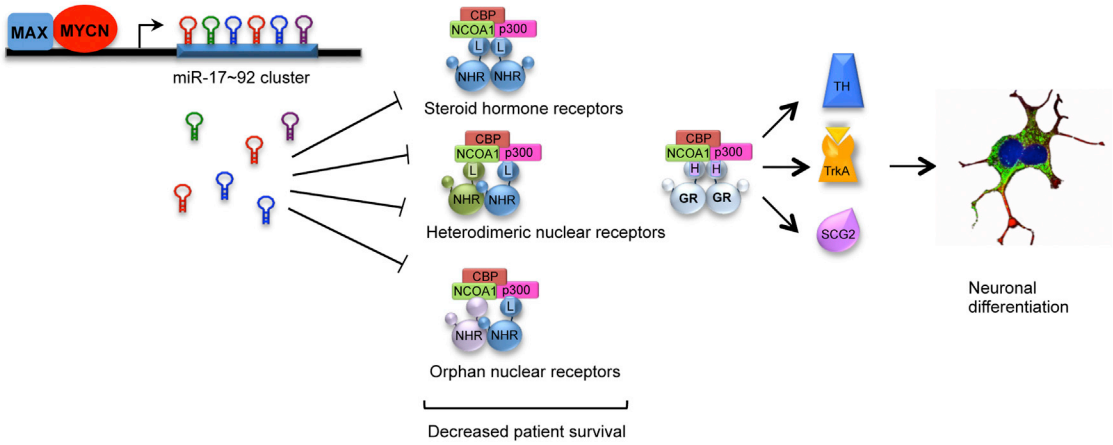

Figure 7. Links among miR-17∼92, NHRs, and Neuroblastoma Patient Outcome

Model illustrating repression of NHR family members by the MYCN-driven miR17∼92 cluster in neuroblastoma. Many NHRs are linked to neuronal differentiation/maturation, and low expression levels are associated with decreased survival in *MYCN*-amplified patients, suggesting that hormonal unresponsiveness may be a contributing factor in neuroblastoma aggressiveness. GR is a direct miR-17∼92 target, which upon activation by DEX stimulates expression of the neuronal differentiation markers TH, TrkA, and SCG2. CBP, cyclic AMP response element-binding protein, a co-activator; GR, glucocorticoid receptor; H, hormone; L, ligand; NCO1A, nuclear co-activator 1; NHR, nuclear hormone receptor; p300: a co-activator; SCG2, secretogranin 2; TH, tyrosine hydroxylase; TrkA, tropomyosin receptor kinase A.

show that GR expression and responsiveness to glucocorticoids is intrinsic to sympathetic neurons and promotes their differentiation. Upon *MYCN* amplification, neuroblasts/neurons that would otherwise express GR fail to initiate or maintain its expression and retain their proliferative status. We further showed that hyperplasias in the ganglia of *TH-MYCN* mice with increased MYCN levels were devoid of GR and of differentiation markers, which were otherwise expressed in the surrounding normal tissue. Moreover, GR signaling led to upregulation of TrkA, SCG2, and TH in vitro, indicating that GR contributes to the differentiation of neural cells.

The current treatment for high-risk patients includes intensive chemotherapy followed by surgery, myeloablative chemotherapy with autologous stem cell rescue, retinoid treatment, and immunotherapy (Øra and Eggert, 2011). Although most patients initially respond to therapy, many succumb to relapse and therapy resistance (Mueller and Matthay, 2009). The differentiation agent 13-*cis* retinoic acid is used as maintenance therapy for high-risk patients in remission (Matthay et al., 2009; Yu et al., 2010). Our in vivo findings reveal that a combined therapeutic approach could be beneficial for neuroblastoma patients. We propose that drugs that disrupt the expression or function of MYCN/MYC or agents that inhibit the miR-17∼92 cluster would render these tumors more responsive to differentiation, thereby promoting hormone treatment (e.g., corticoids). Indeed, alisertib, a highly selective inhibitor of the MYCN-stabilizing aurora A kinase, and miravirsen, a miRNA inhibitor, are already in clinical trials (Brockmann et al., 2013; Janssen et al., 2013). Importantly, DEX is commonly used together with chemotherapy to treat certain types of cancer (Inaba and Pui, 2010; Pui and Evans, 2006). Our findings offer a potential alternative combination therapy that is particularly beneficial for high-risk neuroblastoma patients and that could promptly be translated into a clinical setting.

EXPERIMENTAL PROCEDURES

Detailed materials and methods are provided in the Supplemental Information.

Figure 6. Increased Neural Differentiation and Reduced Tumor Burden upon Activation of GR Signaling

(A) Immunofluorescence of GR in BE(2)-*EV* and BE(2)-*GR* cells. Cells were treated for 6 days where cells were pre-incubated with cumate for 2 days and a combination of cumate and DEX for 4 days. DEX treatment resulted in translocation of cytoplasmic GR into the nucleus. Representative pictures from six experiments are shown. The scale bar represents 25 μm.

(B) Immunoblotting of GR, MYCN, and TH in BE(2)-*GR* cells and in control BE(2)-EV cells with or without induction with cumate in the presence or absence of DEX as indicated. One representative blot from six experiments is shown. α-tubulin was used as loading control.

(C) Quantification of TH by densitometry in BE(2)-EV and BE(2)-*GR* cells. n = 6 with the mean ± SEM is shown for quantification.

(D) Tumor volume index (TVI) in a xenograft model of SK-N-BE(2) neuroblastoma cells, in which the mice were treated with vehicle (DMSO), two different doses of DEX (1 and 10 mg/kg), 10058-F4 (25 mg/kg), or the combination of 10058-F4 pre-treatment followed by 10058-F4 together with 10 mg/kg DEX (10058-F4+DEX10). See Figure S7A for experimental scheme. n = 6 for the vehicle (DMSO), DEX10, 10058-F4, and 10058-F4+DEX10 groups, and n = 5 for the DEX1 group. The mean ± SEM is shown for quantification; *p < 0.05; **p < 0.01; ***p < 0.001; and ****p < 0.0001 compared to vehicle (DMSO).

(E) Tumor weights at the end of treatment. n = 6 for the vehicle (DMSO), DEX10, 10058-F4, and 10058-F4+DEX10 groups; and n = 5 for the DEX1 group. The mean ± SEM is shown for quantification; *p < 0.05.

(F) Quantification of the MYCN levels in all the treated tumors normalized by total protein amount. The mean ± SEM is shown for quantification; *p < 0.05.

(G) Immunohistochemistry for MYCN in tumor sections from treated mice. Three tumors per treatment were analyzed. The scale bar represents 200 μm. Representative sections are presented.

In Silico Prediction and Expression Analysis

TargetScan, PicTar2, miRanda, and mirTarget2 were used for target prediction of miR-17∼92 family members. The NHR score was generated by ranking the seven genes that were predicted targets as well as downregulated in *MYCN*-amplified neuroblastoma patients (*NR3C1*, *NR4A2*, *RORA*, *NR4A3*, *ESR1*, *NR3C2*, and *NCOA1*; Table S6) from lowest to highest across all patients. We employed two gene expression signatures (Fredlund et al., 2008; Valentijn et al., 2012) to infer MYC signaling. All patients were registered in the respective clinical trials with written informed consent from the patient and/or the parents or legal guradian.

Protein Expression

Western blot and immunohistochemistry (IHC) analyses were performed as described (Zirath et al., 2013). For IHC on mouse tissues, 14-μm transverse sections from cryosections were pre-incubated for 1 hr in blocking solution (PBS, 0.25% Triton X-100, and 5% normal goat serum) followed by incubation at 4°C overnight with the primary antibodies diluted in blocking solution. After washing, the slides were incubated for 1–2 hr at room temperature with the appropriate fluorophore-conjugated antibodies. Antibodies are listed in the Supplemental Information.

Animal Experiments

For xenografts studies, 10 × 10^6 SK-N-BE(2) cells were subcutaneously injected in the flanks of nude mice. Tumor take was defined as the point at which tumors reached 0.15 cm^3. Mice were treated for 7 days with vehicle (DMSO), 10058-F4 (25 mg/kg), two different doses of DEX (1 mg/kg and 10 mg/kg), or pretreated with 10058-F4 for 72 hr followed by a combination of 10054-F4 and DEX10 for 4 days (10054-F4+DEX10). As controls, DEX-treated mice were administered DMSO for 72 hr followed by DMSO+DEX10 treatment for 4 days.

NMRI-*Foxn1*^{nu} and *TH-MYCN* were housed, bred, treated, and analyzed in accordance with the permits approved by the Swedish ethical committee Stockholms Norra Djurförsöksetiska Nämnd (ethical approval numbers N231/14 for NMRI-*Foxn1*^{nu} and N26/11, N42/14, and N71/15 for *TH-MYCN*).

SUPPLEMENTAL INFORMATION

Supplemental Information includes Supplemental Experimental Procedures, seven figures, and seven tables and can be found with this article online at http://dx.doi.org/10.1016/j.celrep.2016.06.052.

AUTHOR CONTRIBUTIONS

D.R., M.D.R.K., and U.K.W. performed experiments with help from G.O., J.D., A.K., C.S.B., and J.L. M.D.R.K. and F.H. performed the bioinformatics analyses. M.F. provided patient data and supervised part of the bioinformatics study. P.K. and J.I.J. supervised animal studies. D.R. and M.A.H. designed research, interpreted data, and wrote the manuscript. M.A.H. supervised the study. All authors commented on the manuscript.

ACKNOWLEDGMENTS

We are grateful to Drs. J. Vandesompole (Ghent), M. Schwab (Heidelberg), and J. Shohet (Houston) for cells; Dr. N. Zinin for subcloning; Dr. F. Roels (Cologne) for data analysis; and Drs. E. Fredlund and P. Vlachos for initial bioinformatics and luciferase assays, respectively. We are indebted to Dr. M. Wickström and L. Elfman for animal expertise; A. Magoulopoulou for technical assistance; Dr. J. Goodwin for input on the graphical abstract; Drs. A. Frenzel, M. Stantic, H. Zirath, and M. Wilhelm for discussions; Dr. S. Lain for critical reading of the manuscript; and our groups for helpful comments. We thank the German Neuroblastoma Biobank for tumor samples. M.F. was supported by the Germany Ministry of Science and Education (BMBF) through the e:Med initiative (01ZX1303A and 01ZX1307D) and J.I.J. and P.K. by the Swedish Foundation for Strategic Research. This study was performed with grants from the Swedish Childhood Cancer Foundation, the Swedish Research Council, the Swedish Cancer Society, and Karolinska Institutet (to J.I.J., P.K., and M.A.H.). J.D. and M.A.H. were recipients of a postdoctoral position from the Swedish Childhood Cancer Foundation and of a Senior Investigator Award from the Swedish Cancer Society, respectively.

Received: November 30, 2015
Revised: May 1, 2016
Accepted: June 12, 2016
Published: July 7, 2016

REFERENCES

Albino, D., Brizzolara, A., Moretti, S., Falugi, C., Mirisola, V., Scaruffi, P., Di Candia, M., Truini, M., Coco, S., Bonassi, S., and Tonini, G.P. (2011). Gene expression profiling identifies eleven DNA repair genes down-regulated during mouse neural crest cell migration. Int. J. Dev. Biol. *55*, 65–72.

Balamuth, N.J., Wood, A., Wang, Q., Jagannathan, J., Mayes, P., Zhang, Z., Chen, Z., Rappaport, E., Courtright, J., Pawel, B., et al. (2010). Serial transcriptome analysis and cross-species integration identifies centromere-associated protein E as a novel neuroblastoma target. Cancer Res. *70*, 2749–2758.

Bohn, M.C., McEwen, B., Luine, V.N., and Black, I.B. (1984). Development and characterization of glucocorticoid receptors in rat superior cervical ganglion. Brain Res. *316*, 211–218.

Bookout, A.L., Jeong, Y., Downes, M., Yu, R.T., Evans, R.M., and Mangelsdorf, D.J. (2006). Anatomical profiling of nuclear receptor expression reveals a hierarchical transcriptional network. Cell *126*, 789–799.

Brockmann, M., Poon, E., Berry, T., Carstensen, A., Deubzer, H.E., Rycak, L., Jamin, Y., Thway, K., Robinson, S.P., Roels, F., et al. (2013). Small molecule inhibitors of aurora-a induce proteasomal degradation of N-myc in childhood neuroblastoma. Cancer Cell *24*, 75–89.

Brodeur, G.M. (2003). Neuroblastoma: biological insights into a clinical enigma. Nat. Rev. Cancer *3*, 203–216.

Brodeur, G.M., Nakagawara, A., Yamashiro, D.J., Ikegaki, N., Liu, X.G., Azar, C.G., Lee, C.P., and Evans, A.E. (1997). Expression of TrkA, TrkB and TrkC in human neuroblastomas. J. Neurooncol. *31*, 49–55.

Chawla, A., Repa, J.J., Evans, R.M., and Mangelsdorf, D.J. (2001). Nuclear receptors and lipid physiology: opening the X-files. Science *294*, 1866–1870.

Cochard, P., Goldstein, M., and Black, I.B. (1978). Ontogenetic appearance and disappearance of tyrosine hydroxylase and catecholamines in the rat embryo. Proc. Natl. Acad. Sci. USA *75*, 2986–2990.

Cozzi, M.G., Rosa, P., Greco, A., Hille, A., Huttner, W.B., Zanini, A., and De Camilli, P. (1989). Immunohistochemical localization of secretogranin II in the rat cerebellum. Neuroscience *28*, 423–441.

Edsjö, A., Nilsson, H., Vandesompele, J., Karlsson, J., Pattyn, F., Culp, L.A., Speleman, F., and Påhlman, S. (2004). Neuroblastoma cells with overexpressed MYCN retain their capacity to undergo neuronal differentiation. Lab. Invest. *84*, 406–417.

Finotto, S., Krieglstein, K., Schober, A., Deimling, F., Lindner, K., Brühl, B., Beier, K., Metz, J., Garcia-Arraras, J.E., Roig-Lopez, J.L., et al. (1999). Analysis of mice carrying targeted mutations of the glucocorticoid receptor gene argues against an essential role of glucocorticoid signalling for generating adrenal chromaffin cells. Development *126*, 2935–2944.

Fontana, L., Fiori, M.E., Albini, S., Cifaldi, L., Giovinazzi, S., Forloni, M., Boldrini, R., Donfrancesco, A., Federici, V., Giacomini, P., et al. (2008). Antagomir-17-5p abolishes the growth of therapy-resistant neuroblastoma through p21 and BIM. PLoS ONE *3*, e2236.

Fredlund, E., Ringnér, M., Maris, J.M., and Påhlman, S. (2008). High Myc pathway activity and low stage of neuronal differentiation associate with poor outcome in neuroblastoma. Proc. Natl. Acad. Sci. USA *105*, 14094–14099.

Hansford, L.M., Thomas, W.D., Keating, J.M., Burkhart, C.A., Peaston, A.E., Norris, M.D., Haber, M., Armati, P.J., Weiss, W.A., and Marshall, G.M. (2004). Mechanisms of embryonal tumor initiation: distinct roles for MycN expression and MYCN amplification. Proc. Natl. Acad. Sci. USA *101*, 12664–12669.

Heukamp, L.C., Thor, T., Schramm, A., De Preter, K., Kumps, C., De Wilde, B., Odersky, A., Peifer, M., Lindner, S., Spruessel, A., et al. (2012). Targeted expression of mutated ALK induces neuroblastoma in transgenic mice. Sci. Transl. Med. *4*, 141ra91.

Inaba, H., and Pui, C.H. (2010). Glucocorticoid use in acute lymphoblastic leukaemia. Lancet Oncol. *11*, 1096–1106.

Janssen, H.L., Reesink, H.W., Lawitz, E.J., Zeuzem, S., Rodriguez-Torres, M., Patel, K., van der Meer, A.J., Patick, A.K., Chen, A., Zhou, Y., et al. (2013). Treatment of HCV infection by targeting microRNA. N. Engl. J. Med. *368*, 1685–1694.

Kalinyak, J.E., Dorin, R.I., Hoffman, A.R., and Perlman, A.J. (1987). Tissue-specific regulation of glucocorticoid receptor mRNA by dexamethasone. J. Biol. Chem. *262*, 10441–10444.

Knoepfler, P.S., Cheng, P.F., and Eisenman, R.N. (2002). N-myc is essential during neurogenesis for the rapid expansion of progenitor cell populations and the inhibition of neuronal differentiation. Genes Dev. *16*, 2699–2712.

Kocak, H., Ackermann, S., Hero, B., Kahlert, Y., Oberthuer, A., Juraeva, D., Roels, F., Theissen, J., Westermann, F., Deubzer, H., et al. (2013). Hox-C9 activates the intrinsic pathway of apoptosis and is associated with spontaneous regression in neuroblastoma. Cell Death Dis. *4*, e586.

Kogner, P., Barbany, G., Dominici, C., Castello, M.A., Raschellá, G., and Persson, H. (1993). Coexpression of messenger RNA for TRK protooncogene and low affinity nerve growth factor receptor in neuroblastoma with favorable prognosis. Cancer Res. *53*, 2044–2050.

Li, L., Hung, A.C., and Porter, A.G. (2008). Secretogranin II: a key AP-1-regulated protein that mediates neuronal differentiation and protection from nitric oxide-induced apoptosis of neuroblastoma cells. Cell Death Differ. *15*, 879–888.

Lovén, J., Zinin, N., Wahlström, T., Müller, I., Brodin, P., Fredlund, E., Ribacke, U., Pivarcsi, A., Påhlman, S., and Henriksson, M. (2010). MYCN-regulated microRNAs repress estrogen receptor-alpha (ESR1) expression and neuronal differentiation in human neuroblastoma. Proc. Natl. Acad. Sci. USA *107*, 1553–1558.

Lutz, W., Stöhr, M., Schürmann, J., Wenzel, A., Löhr, A., and Schwab, M. (1996). Conditional expression of N-myc in human neuroblastoma cells increases expression of alpha-prothymosin and ornithine decarboxylase and accelerates progression into S-phase early after mitogenic stimulation of quiescent cells. Oncogene *13*, 803–812.

Mangelsdorf, D.J., Thummel, C., Beato, M., Herrlich, P., Schütz, G., Umesono, K., Blumberg, B., Kastner, P., Mark, M., Chambon, P., and Evans, R.M. (1995). The nuclear receptor superfamily: the second decade. Cell *83*, 835–839.

Maris, J.M. (2010). Recent advances in neuroblastoma. N. Engl. J. Med. *362*, 2202–2211.

Matthay, K.K., Reynolds, C.P., Seeger, R.C., Shimada, H., Adkins, E.S., Haas-Kogan, D., Gerbing, R.B., London, W.B., and Villablanca, J.G. (2009). Long-term results for children with high-risk neuroblastoma treated on a randomized trial of myeloablative therapy followed by 13-cis-retinoic acid: a children's oncology group study. J. Clin. Oncol. *27*, 1007–1013.

Mestdagh, P., Boström, A.K., Impens, F., Fredlund, E., Van Peer, G., De Antonellis, P., von Stedingk, K., Ghesquière, B., Schulte, S., Dews, M., et al. (2010). The miR-17-92 microRNA cluster regulates multiple components of the TGF-β pathway in neuroblastoma. Mol. Cell *40*, 762–773.

Meyer, J.S. (1983). Early adrenalectomy stimulates subsequent growth and development of the rat brain. Exp. Neurol. *82*, 432–446.

Meyer, J.S. (1985). Biochemical effects of corticosteroids on neural tissues. Physiol. Rev. *65*, 946–1020.

Mueller, S., and Matthay, K.K. (2009). Neuroblastoma: biology and staging. Curr. Oncol. Rep. *11*, 431–438.

Müller, I., Larsson, K., Frenzel, A., Oliynyk, G., Zirath, H., Prochownik, E.V., Westwood, N.J., and Henriksson, M.A. (2014). Targeting of the MYCN protein with small molecule c-MYC inhibitors. PLoS ONE *9*, e97285.

Munier, M., Meduri, G., Viengchareun, S., Leclerc, P., Le Menuet, D., and Lombès, M. (2010). Regulation of mineralocorticoid receptor expression during neuronal differentiation of murine embryonic stem cells. Endocrinology *151*, 2244–2254.

O'Donnell, K.A., Wentzel, E.A., Zeller, K.I., Dang, C.V., and Mendell, J.T. (2005). c-Myc-regulated microRNAs modulate E2F1 expression. Nature *435*, 839–843.

Onate, S.A., Boonyaratanakornkit, V., Spencer, T.E., Tsai, S.Y., Tsai, M.J., Edwards, D.P., and O'Malley, B.W. (1998). The steroid receptor coactivator-1 contains multiple receptor interacting and activation domains that cooperatively enhance the activation function 1 (AF1) and AF2 domains of steroid receptors. J. Biol. Chem. *273*, 12101–12108.

Øra, I., and Eggert, A. (2011). Progress in treatment and risk stratification of neuroblastoma: impact on future clinical and basic research. Semin. Cancer Biol. *21*, 217–228.

Ozawa, H., and Takata, K. (1995). The granin family–its role in sorting and secretory granule formation. Cell Struct. Funct. *20*, 415–420.

Pandey, D.P., and Picard, D. (2010). Multidirectional interplay between nuclear receptors and microRNAs. Curr. Opin. Pharmacol. *10*, 637–642.

Parlato, R., Otto, C., Tuckermann, J., Stotz, S., Kaden, S., Gröne, H.J., Unsicker, K., and Schütz, G. (2009). Conditional inactivation of glucocorticoid receptor gene in dopamine-beta-hydroxylase cells impairs chromaffin cell survival. Endocrinology *150*, 1775–1781.

Polman, J.A., Welten, J.E., Bosch, D.S., de Jonge, R.T., Balog, J., van der Maarel, S.M., de Kloet, E.R., and Datson, N.A. (2012). A genome-wide signature of glucocorticoid receptor binding in neuronal PC12 cells. BMC Neurosci. *13*, 118.

Pui, C.H., and Evans, W.E. (2006). Treatment of acute lymphoblastic leukemia. N. Engl. J. Med. *354*, 166–178.

Rada-Iglesias, A., Bajpai, R., Prescott, S., Brugmann, S.A., Swigut, T., and Wysocka, J. (2012). Epigenomic annotation of enhancers predicts transcriptional regulators of human neural crest. Cell Stem Cell *11*, 633–648.

Rasmuson, A., Segerström, L., Nethander, M., Finnman, J., Elfman, L.H., Javanmardi, N., Nilsson, S., Johnsen, J.I., Martinsson, T., and Kogner, P. (2012). Tumor development, growth characteristics and spectrum of genetic aberrations in the TH-MYCN mouse model of neuroblastoma. PLoS ONE *7*, e51297.

Sacchetti, P., Sousa, K.M., Hall, A.C., Liste, I., Steffensen, K.R., Theofilopoulos, S., Parish, C.L., Hazenberg, C., Richter, L.A., Hovatta, O., et al. (2009). Liver X receptors and oxysterols promote ventral midbrain neurogenesis in vivo and in human embryonic stem cells. Cell Stem Cell *5*, 409–419.

Schulte, J.H., Horn, S., Otto, T., Samans, B., Heukamp, L.C., Eilers, U.C., Krause, M., Astrahantseff, K., Klein-Hitpass, L., Buettner, R., et al. (2008). MYCN regulates oncogenic microRNAs in neuroblastoma. Int. J. Cancer *122*, 699–704.

Slack, A., Lozano, G., and Shohet, J.M. (2005). MDM2 as MYCN transcriptional target: implications for neuroblastoma pathogenesis. Cancer Lett. *228*, 21–27.

Smith, J., and Fauquet, M. (1984). Glucocorticoids stimulate adrenergic differentiation in cultures of migrating and premigratory neural crest. J. Neurosci. *4*, 2160–2172.

Steiner, H.J., Schmid, K.W., Fischer-Colbrie, R., Sperk, G., and Winkler, H. (1989). Co-localization of chromogranin A and B, secretogranin II and neuropeptide Y in chromaffin granules of rat adrenal medulla studied by electron microscopic immunocytochemistry. Histochemistry *91*, 473–477.

Stergiopoulos, A., and Politis, P.K. (2013). The role of nuclear receptors in controlling the fine balance between proliferation and differentiation of neural stem cells. Arch. Biochem. Biophys. *534*, 27–37.

Tata, J.R. (2002). Signalling through nuclear receptors. Nat. Rev. Mol. Cell Biol. *3*, 702–710.

Terrile, M., Bryan, K., Vaughan, L., Hallsworth, A., Webber, H., Chesler, L., and Stallings, R.L. (2011). miRNA expression profiling of the murine TH-MYCN neuroblastoma model reveals similarities with human tumors and identifies novel candidate miRNAs. PLoS ONE *6*, e28356.

Valentijn, L.J., Koster, J., Haneveld, F., Aissa, R.A., van Sluis, P., Broekmans, M.E., Molenaar, J.J., van Nes, J., and Versteeg, R. (2012). Functional MYCN

signature predicts outcome of neuroblastoma irrespective of MYCN amplification. Proc. Natl. Acad. Sci. USA *109*, 19190–19195.

Vreugdenhil, E., Verissimo, C.S., Mariman, R., Kamphorst, J.T., Barbosa, J.S., Zweers, T., Champagne, D.L., Schouten, T., Meijer, O.C., de Kloet, E.R., and Fitzsimons, C.P. (2009). microRNA 18 and 124a down-regulate the glucocorticoid receptor: implications for glucocorticoid responsiveness in the brain. Endocrinology *150*, 2220–2228.

Wakamatsu, Y., Watanabe, Y., Nakamura, H., and Kondoh, H. (1997). Regulation of the neural crest cell fate by N-myc: promotion of ventral migration and neuronal differentiation. Development *124*, 1953–1962.

Weiss, W.A., Aldape, K., Mohapatra, G., Feuerstein, B.G., and Bishop, J.M. (1997). Targeted expression of MYCN causes neuroblastoma in transgenic mice. EMBO J. *16*, 2985–2995.

Westermann, F., Muth, D., Benner, A., Bauer, T., Henrich, K.O., Oberthuer, A., Brors, B., Beissbarth, T., Vandesompele, J., Pattyn, F., et al. (2008). Distinct transcriptional MYCN/c-MYC activities are associated with spontaneous regression or malignant progression in neuroblastomas. Genome Biol. *9*, R150.

Xu, J., and Li, Q. (2003). Review of the in vivo functions of the p160 steroid receptor coactivator family. Mol. Endocrinol. *17*, 1681–1692.

Xu, J., Wu, R.C., and O'Malley, B.W. (2009). Normal and cancer-related functions of the p160 steroid receptor co-activator (SRC) family. Nat. Rev. Cancer *9*, 615–630.

Yin, X., Giap, C., Lazo, J.S., and Prochownik, E.V. (2003). Low molecular weight inhibitors of Myc-Max interaction and function. Oncogene *22*, 6151–6159.

Yu, A.L., Gilman, A.L., Ozkaynak, M.F., London, W.B., Kreissman, S.G., Chen, H.X., Smith, M., Anderson, B., Villablanca, J.G., Matthay, K.K., et al.; Children's Oncology Group (2010). Anti-GD2 antibody with GM-CSF, interleukin-2, and isotretinoin for neuroblastoma. N. Engl. J. Med. *363*, 1324–1334.

Zetterström, R.H., Solomin, L., Jansson, L., Hoffer, B.J., Olson, L., and Perlmann, T. (1997). Dopamine neuron agenesis in Nurr1-deficient mice. Science *276*, 248–250.

Zimmerman, K.A., Yancopoulos, G.D., Collum, R.G., Smith, R.K., Kohl, N.E., Denis, K.A., Nau, M.M., Witte, O.N., Toran-Allerand, D., Gee, C.E., et al. (1986). Differential expression of myc family genes during murine development. Nature *319*, 780–783.

Zirath, H., Frenzel, A., Oliynyk, G., Segerström, L., Westermark, U.K., Larsson, K., Munksgaard Persson, M., Hultenby, K., Lehtiö, J., Einvik, C., et al. (2013). MYC inhibition induces metabolic changes leading to accumulation of lipid droplets in tumor cells. Proc. Natl. Acad. Sci. USA *110*, 10258–10263.